AIP | Applied Physics Letters

Aluminum plasmonic nanostructures for improved absorption in organic photovoltaic devices

Vladimir Kochergin, Lauren Neely, Chih-Yu Jao, and Hans D. Robinson

Citation: Applied Physics Letters **98**, 133305 (2011); doi: 10.1063/1.3574091
View online: http://dx.doi.org/10.1063/1.3574091
View Table of Contents: http://scitation.aip.org/content/aip/journal/apl/98/13?ver=pdfcov
Published by the AIP Publishing

Aluminum plasmonic nanostructures for improved absorption in organic photovoltaic devices

Vladimir Kochergin,[1,a)] Lauren Neely,[1] Chih-Yu Jao,[2] and Hans D. Robinson[2]
[1]*MicroXact, Inc., Blacksburg, Virginia 24060, USA*
[2]*Department of Physics, Virginia Tech, Blacksburg, Virginia 24060, USA*

(Received 18 February 2011; accepted 13 March 2011; published online 31 March 2011)

We model the absorption enhancement in organic photovoltaic devices induced by incorporating Al, Ag, and Au nanoparticles in the active layer. We find that Al nanoparticles should yield significantly greater enhancement than Ag or Au. This is because the much higher plasma frequency of Al ensures a better overlap between plasmon resonance and absorption band of organic semiconductors. Our predictions are verified experimentally by demonstrating enhanced absorbance in a poly(3-hexylthiophene-2,5-diyl): [6,6]-phenyl C61 butyric acid methyl ester layer with embedded functionalized Al nanoparticles. © *2011 American Institute of Physics*.
[doi:10.1063/1.3574091]

Organic Photovoltaics (OPV) have several advantages over their inorganic counterparts, particularly, in terms of fabrication costs and application versatility.[1] However, their energy conversion efficiencies are at present significantly below those in inorganic materials. The OPV efficiency is mostly limited by intrinsic material properties; the high energy and narrow spectral range of the absorption band results in inefficient harvesting of solar radiation, while low carrier mobilities limit the active layer thickness. As a result, thin active layers are inefficient due to poor absorbance, and thicker ones are inefficient due to bulk recombination losses. Work over the past decade, recently reviewed by Atwater and Polman,[2] has attempted to resolve this conflict by placing plasmonic structures in or around the OPV active layer. This has the potential to significantly enhance the electromagnetic (EM) field in the active layer, either because of the strong scattering provided by the plasmonic nanostructures or by direct overlap between the intense field of the plasmon modes and the active layer. This in turn generates a much improved light absorption without requiring a thicker active layer, and thus a higher efficiency PV cell.

One of the more promising results to date is a 70% efficiency enhancement that was observed in a poly(3-hexylthiophene-2,5-diyl): [6,6]-phenyl C61 butyric acid methyl ester (P3HT:PCBM) OPV device with Ag nanoparticles (NPs) distributed near the surface of the active layer,[3] although both initial and enhanced conversion efficiencies (1.3% and 2.2%) were well below the state of the art for this material system. Enhancements in the short-circuit current density in P3HT:PCBM OPV devices utilizing Ag nanohole backside electrodes[4] or Au nanopillar arrays at the active layer interface[5] have also been demonstrated, although no enhancement of the conversion efficiency was reported. A significant *degradation* of the conversion efficiencies in P3HT:PCBM OPV devices were observed when Au NPs were embedded into the active layer.[6] So the promise of plasmonics to strongly improve OPV efficiencies remains unfulfilled. Experimental results are also often contradictory to theoretical predictions, leaving many questions open for further study.

In this letter, we aim to advance the understanding of this issue by modeling the absorbance enhancement achieved by embedding Au, Ag, and Al NPs in OPV active layers. Our analysis shows that both Au and Ag are nonoptimal for the purposes of enhancing OPV efficiencies, while Al offers much better performance. We also present preliminary experimental results to validate this conclusion.

For our analysis, we chose P3HT:PCBM (1:1) and poly [2,6-(4,4-bis - (2-ethylhexyl) - 4H-cyclopenta [2,1-b; 3,4-b′]-dithiophene)-alt-4,7-(2,1,3-benzothiadiazole) (PCPDTBT): C_{70}-PCBM (1:1) as the active layer materials. P3HT:PCBM is the best-studied of the OPV materials, while PCPDTBT:PCBM is emerging as one of the most promising materials for high efficiency OPV.[7] We estimated the absorption in the nanocomposites using Bruggeman's effective medium approximation (EMA).[8] This model is reasonably accurate at low metal concentrations and easy to implement. For P3HT:PCBM (1:1) we used previously published dielectric constants,[9] while for PCPDTBT:PCBM (1:1) we retrieved the dielectric constants by fitting published absorbance data[10] under the assumption that the real part of the refractive index is close to that of P3HT:PCBM. We used published optical constants for Au,[11] Ag,[11] and Al.[12] We accounted neither for changes in metal dielectric constants at the small NP diameter limit nor for retardation effects. All NPs were assumed to be spherical.

We simulated the EM field enhancement factors for various concentrations of Al, Ag, and Au NPs in P3HT:PCBM (1:1) matrix [Fig. 1(a)] and PCPDYBT:C_{70}-PCBM matrix [Fig. 1(b)]. The normalized absorbances of the matrix materials are also plotted in Fig. 1. We see that even very small concentrations of Au NPs shifts the plasmonic peak to wavelengths beyond the absorption band of P3HT:PCBM and barely overlapping with the absorption band edge of the PCPDTBT:C_{70}-PCBM. Au NPs should therefore not yield any efficiency enhancement in OPV cells, in line with experimental results by Topp *et al.*[6] For Ag NPs, the plasmonic peak is also outside of the P3HT:PBCM absorption band, but a reasonable overlap with the absorption band of PCPDTBT:C_{70}-PCBM is predicted for particle concentrations below 3%. When that happens, the strong absorption of the polymer degrades the plasmon resonance, which mani-

a)Electronic mail: vkochergin@microxact.com.

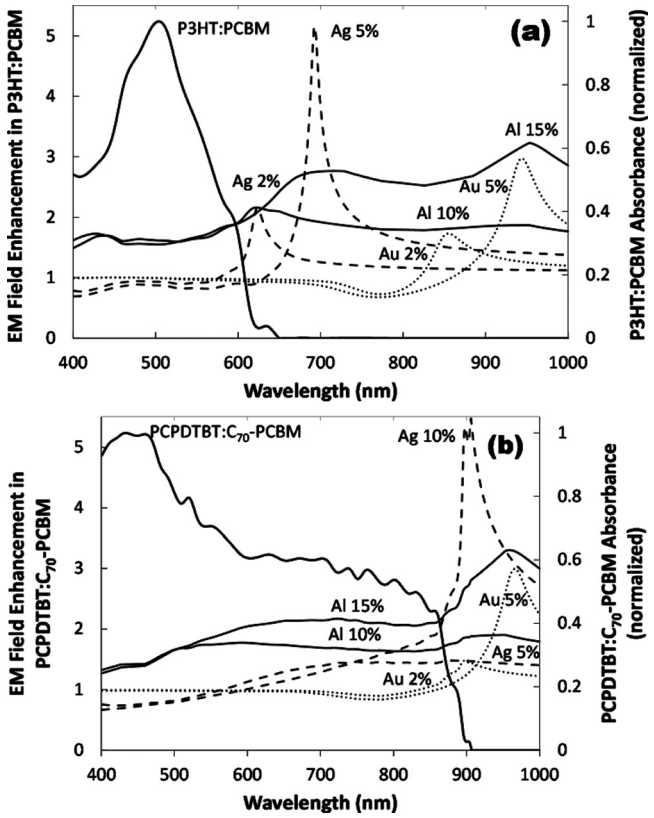

FIG. 1. Calculated EM field enhancement spectra in (a) P3HT:PCBM (1:1) and (b) PCPDTBT:C_{70}-PCBM (1:1) organic semiconductor/metal nanocomposites for varying volumetric loadings of Al (thin solid lines), Ag (dashed), and Au (dotted) NPs. The thick solid lines in (a) and (b) show the calculated absorption spectra of P3HT:PCBM (1:1) and PCPDTBT:C_{70}-PCBM (1:1), respectively.

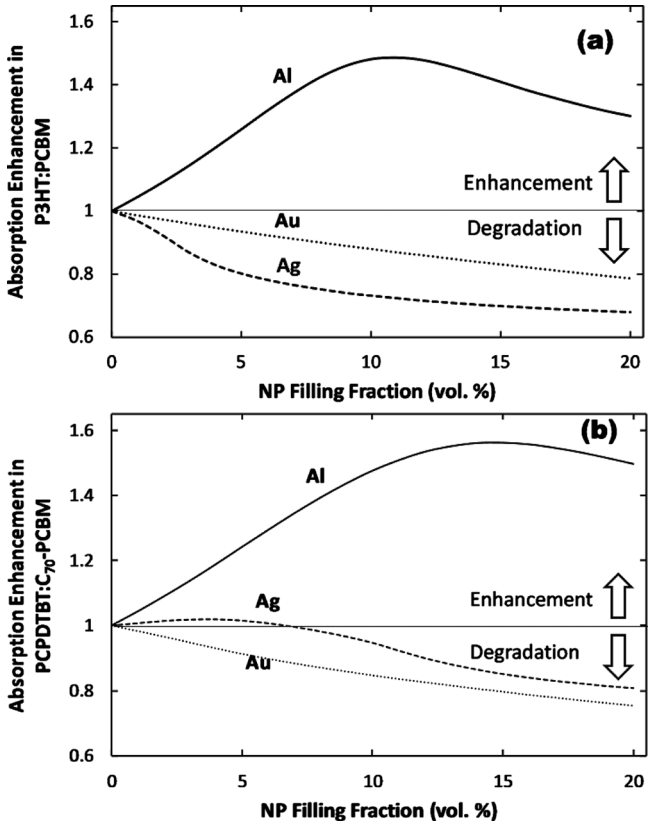

FIG. 2. Calculated absorbance enhancements in (a) P3HT:PCBM (1:1)- and (b) PCPDTBT:C_{70}-PCBM (1:1)-metal NPs nanocomposites vs volumetric filling fractions of Al, Ag, and Au NPs.

fests as a marked broadening and weakening of the plasmon peak. Al has a much higher plasma frequency (~15.3 eV) than Ag (9.6 eV) and Au (8.55eV), which causes the Al NP enhancement peak to overlap well with the absorption bands of both P3HT:PCBM and PCPDTBT:C_{70}-PCBM, even at high NP concentrations.

Figure 2 shows the calculated absorption enhancement in P3HT:PCBM:NP [Fig. 2(a)] and PCPDTBT:C_{70}-PCBM:NP [Fig. 2(b)] nanocomposites versus metal NP loading for Al, Ag, and Au NPs. The trends discussed in relation to Fig. 1 are clearly visible: Poor overlap between the plasmonic band of Au and Ag NPs and the P3HT:PCBM absorption band results in reduction in the absorption in P3HT:PCBM (the particles effectively screen the P3HT:PCBM material). Al NPs, on the other hand, are predicted to improve absorbance in P3HT:PCBM by as much as 50% at ~11% volumetric filling fraction. A better overlap between the Ag NP plasmonic band and PCPDTBT:C_{70}-PCBM absorption band results in a small increase in the absorbance around a 4% filling fraction. The optimum loading of Al NPs in PCPDTBT:C_{70}-PCBM is about 15%, resulting in a much larger absorption enhancement of nearly 60%.

It should be noted that these enhancements do not automatically translate into enhancements in PV conversion efficiency. Metal NPs often cause significant losses associated with exciton recombination when embedded in an organic semiconductor. This process is not well understood, and is strongly dependent on NPs functionalization.[6] Strategies to cope with this problem include placing NPs at the interface of the active layer rather than embedded within it, and selecting a NP capping layer that minimally disrupts the excitons in the organic semiconductor.

To verify our model, we measured the light absorbance in P3HT:PCBM films with and without embedded Al NPs. Since Al NPs of sufficient stability against oxidation are not commercially available, we synthesized them following a procedure by Meziani *et al.*[13] Briefly, alane N,N-dimethylethylamine ($H_3AlN(CH_3)_2C_2H_5$) was catalytically decomposed into metallic aluminum under inert conditions in the presence of octadecanoic acid. The acid chelates onto the surface of the Al NPs, limiting their size and protecting them from oxidation.

The particles were characterized with scanning electron microscopy (SEM) imaging (see inset in Fig. 3), ^{13}C solid state NMR and thermogravimetric analysis (TGA). Imaging showed particle size to be below 200 nm, the NMR results confirmed that octadecanoic acid bonded to the Al surface, while TGA confirmed improved stability of the particles, as the functionalized particles contained ~55% metallic aluminum by weight compared to ~26.5% for unfunctionalized particles after a similar amount of air exposure.

Two P3HT:PCBM (1:1) films, identically prepared except one was loaded with ~10 vol % Al NPs were spin-coated onto glass slides. The absorption spectra measured in these films are shown in Fig. 3 together with the best fits to our model and the measured absorption spectrum of our Al NPs. The fit is consistent with 13% NPs in the film, reasonably close to the correct value.

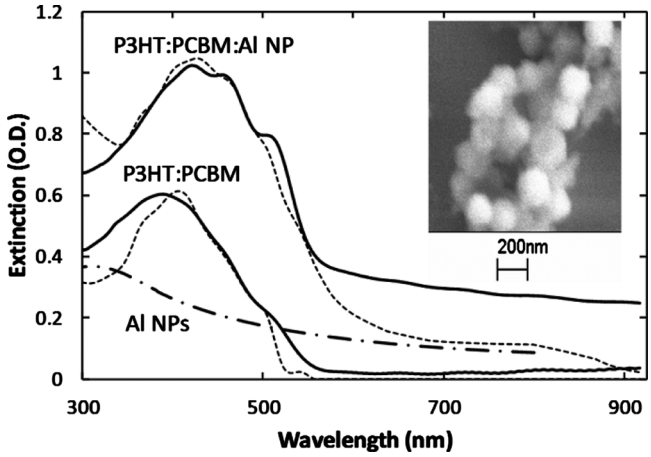

FIG. 3. Absorption spectra of thin films of P3HT:PCBM (1:1) and P3HT:PCBM (1:1) with embedded Al NPs functionalized with octadecanoic acid near 10% volumetric filling fraction (solid curves) together with numerically calculated using developed model absorption curves for P3HT:PCBM (1:1) and P3HT:PCBM (1:1) with embedded Al NPs at 13% volumetric filling fraction (dashed curves). The dashed-dotted curve is the measured absorption spectrum of dilute Al NPs. Inset: SEM image of Al NPs stabilized with an octadecanoic acid capping layer.

The discrepancy between model and data for the particle-free P3HT:PCBM control film both at short and long wavelengths indicate inaccuracies in the optical constants for P3HT:PCBM used in the model.[9] Similarly, a mismatch between the tabulated values of the dielectric function in bulk Al and the actual values for the Al NPs lead to additional discrepancies below 350 nm. The significantly underestimated red tail in the spectrum for the P3HT:PCBM:Al NP film is inherent in the EMA model,[8] and is due to neglecting multipolar interactions.[14] This approximation leads to an underestimation of the redshift in the plasmon band with particle concentration, and is the likely cause of the overestimation of the Al NP concentration. We also need to mention that the incorporation of Al NPs in the film leads to considerable roughness, making it difficult to determine the extent to which both films contain the same amount of organic semiconductor. This is obviously a source of additional uncertainties.

Still, the good fit between model and preliminary data lends credence to our model and supports our conclusion that Al NPs are superior to their Au and Ag counterparts in enhancing the light absorption in OPV active layers, and thus likely to bring about significant improvements in the conversion efficiency of OPV devices. This stems from the high plasma frequency of Al, which permits the use of particle concentrations close to the percolation threshold, enabling greater absorption enhancement while maintaining good overlap between the plasmon resonance and the natural absorption bands of the OPV materials. In addition, while the Al NP synthesis still needs to be perfected, our preliminary work already points to the feasibility of making Al NPs of well-controlled sizes that are stable against oxidation.

This research is supported by AFOSR STTR Contract No. FA9550-10-C-0059. We would like to thank Dr. Sungsool Wi for sharing the solid state NMR data, and also Dr. Dave Dillard for giving us access to his thermogravimetric analyzer.

[1]S. R. Forrest, MRS Bull. **30**, 28 (2005).
[2]H. A. Atwater and A. Polman, Nature Mater. **9**, 205 (2010).
[3]A. J. Morfa, K. L. Rowlen, T. H. Reilly III, M. J. Romero, and J. van de Lagemaat, Appl. Phys. Lett. **92**, 013504 (2008).
[4]W. L. Bai, Q. Q. Gan, G. F. Song, L. H. Chen, Z. Kafafi, and F. Bartoli, Opt. Express **18**, A620 (2010).
[5]S.-J. Tsai, M. Ballarotto, D. B. Romero, W. N. Herman, H. C. Kan, and R. J. Phaneuf, Opt. Express **18**, A528 (2010).
[6]K. Topp, H. Borchert, F. Johnen, A. V. Tunc, M. Knipper, E. von Hauff, J. Parisi, and K. Al-Shamery, J. Phys. Chem. A **114**, 3981 (2010).
[7]D. Mühlbacher, M. Scharber, M. Morana, Z. G. Zhu, D. Waller, R. Gaudiana, and C. Brabec, Adv. Mater. (Weinheim, Ger.) **18**, 2884 (2006).
[8]D. A. G. Bruggeman, Ann. Phys. **416**, 636 (1935).
[9]H. H. Shen, P. Bienstman, and B. Maes, J. Appl. Phys. **106**, 073109 (2009).
[10]M. Koppe, H.-J. Egelhaaf, G. Dennler, M. C. Scharber, C. J. Brabec, P. Schilinsky, C. N. Hoth, Adv. Funct. Mater. **20**, 338 (2010).
[11]P. B. Johnson and R. W. Christy, Phys. Rev. B **6**, 4370 (1972).
[12]E.F. Schubert, 2004, Refractive index and extinction coefficient of materials, http://www.rpi.edu/~schubert/Educational-resources/Materials-Refractive-index-and-extinction-coefficient.pdf (March 28, 2011).
[13]M. J. Meziani, C. E. Bunker, F. S. Lu, H. T. Li, W. Wang, E. A. Guliants, R. A. Quinn, and Y. P. Sun, ACS Appl. Mater. Interfaces **1**, 703 (2009).
[14]V. Kochergin, V. Zaporojtchenko, H. Takele, F. Faupel, and H. Föll, J. Appl. Phys. **101**, 024302 (2007).